A Numerical Study of Topographic Wave Reflection in Semi-infinite Channels

THOMAS STOCKER

Eidgenössische Technische Hochschule, Zürich, Switzerland

(Manuscript received 7 July 1987, in final form 30 October 1987)

ABSTRACT

The potential vorticity equation describing topographic waves is approximately solved using the channel method of Stocker and Hutter. The domain of integration is a semi-infinite channel and models an estuary, the bathymetry of which is varied through a transverse and a longitudinal topography parameter. It is shown that in this domain the spectrum of topographic waves consists of a discrete and a continuous part. The former exhibits wave modes trapped at the closed end of the channel; these waves correspond to the bay modes in a rectangular basin. Resonances with a similar bay-trapped structure also occur in the continuous spectrum. Their dependence on the bay geometry is studied. A consistent explanation of the three topographic wave types found earlier in an enclosed basin is given in terms of topographic wave reflections.

1. Introduction

In the last decades it became clear that a remarkable amount of kinetic energy of water motion in ocean bays and lakes is embodied in long-periodic waves. These are due to (i) the local component of Earth's rotation and (ii) variable water depth, and the wave generating mechanism is the conservation of potential vorticity. The most prominent example of these topographic, or second class, waves is the rotational motion along the continental shelves (shelf waves), of which the properties have extensively been studied, Mysak (1980). Also, in channels and enclosed lake basins, these waves could be detected and observational results have satisfactorily been interpreted by analytical models. For an overview we refer to Stocker and Hutter (1987b, henceforth SH).

Johnson (1987b) and SH (1987a) pointed out that the interpretation of long-periodic signals in the northern basin of the Swiss Lake Lugano in the range of 70 to 80 hours—the fundamental internal gravity mode has $T = 24$ h—in terms of fundamental topographic wave modes was unsatisfactory. Further, finite element solutions (Trösch, 1984) revealed that basin wide modes only exist for far longer periods ($T > 150$ h) whereas solutions in the time range of interest exhibit characteristic patterns. They consist of wave motion localised in the bays of the elongated lake and are rapidly evanescent away from the bays (see later however). Such modes could also be found in rectangular model lakes (SH, 1987a); yet their physical nature was not clear. This can be illuminated by considering topographic waves in semi-infinite channels.

Until now, only a precursory study of reflected topographic waves in semi-infinite channels was presented by SH (1986). The reflection was induced by a vertical end wall. It turned out that these configurations were too simple and did not fully account for the characteristics of topographic wave motion. Nevertheless, a semi-infinite channel, with an appropriate depth profile is a geometry of importance. With it, a gap in the theoretical knowledge of second-class wave propagation can be filled. A further step toward understanding the propagation of topographic waves in semi-infinite channels was made by Johnson (1987b). The study employs the invariance property of the linear barotropic potential vorticity equation under conformal mapping. A half-plane is mapped onto a semi-infinite channel. As the solutions in the former configuration can be constructed for an exponential shelf profile, results are also available for the latter. Physically, however, these solutions must be regarded as describing only a particular reflection process. The incoming wave is mathematically identical with the reflected wave. Presently no allowance is made for a more general situation when evanescent modes occur or wave energy is distributed onto other propagating modes in the course of reflection. Thus, so far the conformal mapping technique yields geometries that exhibit perfect transmission of incident wave energy.

It was recently shown (SH, 1987a) that topographic waves in a rectangular basin may structurally be very rich. Figure 1 depicts contour lines of the streamfunctions of several eigenmodes in a 2:1 basin. Generally, three types can be distinguished: Ball-modes (type 1), well known from analytic models, channel-modes (type 3) which mathematically are related to the former and,

Corresponding author address: Dr. Thomas Stocker, Eidgenossische Technische Hochschule, ETH-Zentrum, CH-8092 Zurich, Switzerland.

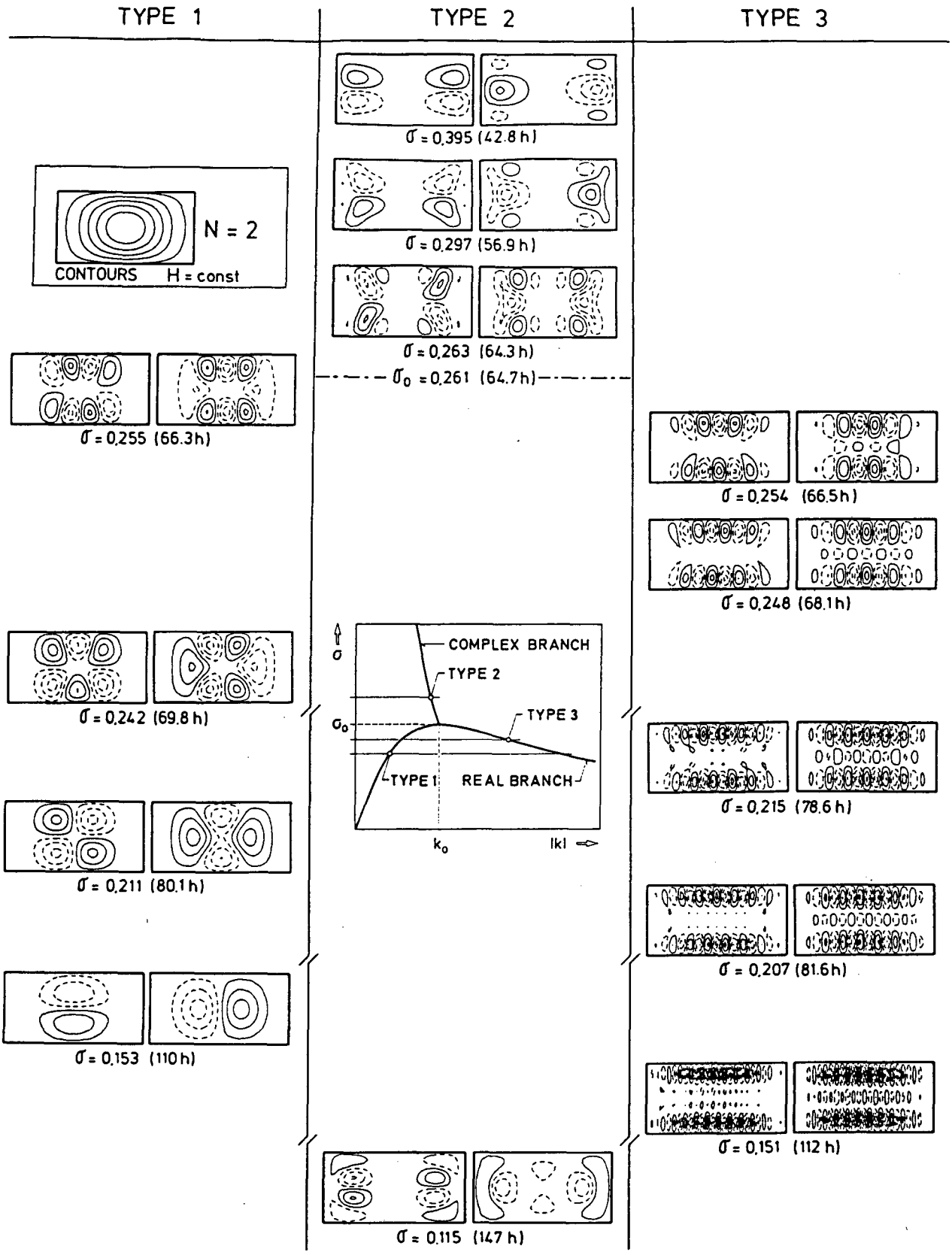

FIG. 1. Selection through the spectrum of topographic wave modes in a second-order model. The eigenfrequencies increase towards the top of the figure. The contour lines of ψ are plotted for time $t = 0$ (left) and $t = T/4$ (right). Three types of solutions can be distinguished and cuts of the vertical lines indicate further modes not shown here. The inset displays the dipersion relation for the straight infinite channel. (From Stocker and Hutter, 1987a.)

more interesting, bay-modes (type 2). The frequencies of the fundamental bay-modes exceed the cutoff σ_0 above which there is no free wave propagation in the infinite channel. These modes show wave motion which is trapped in the lake ends. The longer a lake is, the weaker will be the interaction and coupling of the two bay-modes. So we wondered whether these bay-modes could also exist in semi-infinite domains. The above classification into three mode types was introduced on the basis of phenomenological arguments and a correspondence to the dispersion relation of topographic waves in an infinite channel was shown. Here we intend to demonstrate that it can be put on a *physical* foundation.

Likewise, the problem of a gravity wave modified by the Earth's rotation, a Kelvin wave, propagating in a straight channel and hitting a reflecting wall was analytically solved by Taylor (1920). The result was that the incident Kelvin wave was transformed into a reflected Kelvin wave traveling backward and a series of spatially evanescent or oscillating Poincaré modes. Complete reflection prevails if the frequency is larger than the cutoff for the Poincaré modes. This case was studied by Brown (1973). It is shown here that an incident topographic wave analogously evolves in a series of different reflected modes.

In section 2 the governing equations, boundary and asymptotic conditions are explained. Section 3 gives reflection patterns and parameter dependencies are investigated. It is shown that the three types of topographic waves can be understood in terms of wave reflections.

2. Mathematical model

The motion of topographic waves is best described by the principle of the conservation of potential vorticity. With the assumption of a homogeneous water body and by invoking the rigid-lid and the f-plane approximations, the linearized, time-free potential vorticity equation takes the form

$$[i\sigma\nabla\cdot H^{-1}\nabla + \mathbf{z}\cdot\nabla H^{-1}\times\nabla]\psi = 0, \quad \text{in } \mathcal{D} \tag{2.1}$$

where $\sigma = \omega/f$ is the dimensionless frequency, f the Coriolis parameter, ψ the barotropic mass transport streamfunction, H the water depth, ∇ the horizontal gradient operator and $\mathbf{z}$ the vertical unit vector. The vertically averaged velocity field is obtained from the streamfunction by evaluating

$$\mathbf{u} = H^{-1}(\mathbf{z}\times\nabla\psi). \tag{2.2}$$

The domain of interest is an estuary the geometry of which is shown in Fig. 2. The natural coordinate system (s, n, z) has a straight n-axis and the curved s-axis follows the surface projection of the thalweg. We assume a width $B(s)$, a local radius of curvature $\kappa^{-1}(s)$ and symmetric cross sections such that $H(s, n) = H(s, -n)$. More specifically, we choose

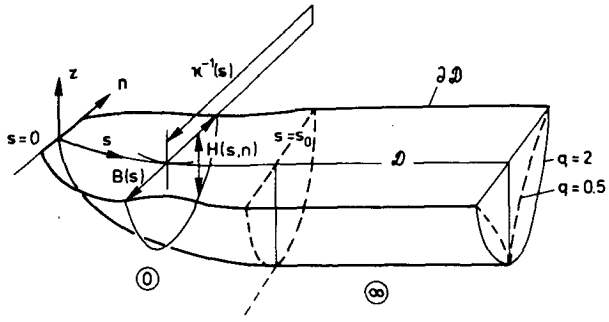

FIG. 2. Estuary domain $\mathcal{D}$ with open boundary $\partial\mathcal{D}$ in a natural coordinate system (s, n, z). Cross sections are symmetric with respect to n and have width $B(s)$. The shore zone ⓪ $0 < s < s_0$ joins at s_0 a straight, infinite channel ∞ with constant cross sections.

$$H(s, n) = h(s)\left(1 + \epsilon - \left|\frac{2n}{B(s)}\right|^q\right),$$

with the sidewall parameter ϵ and the transverse topography parameter q allowing for convex ($q < 1$) and concave ($q > 1$) profiles. The shore- or bay-zone $0 < s < s_0$ joins a straight, infinite channel of constant width and thalweg depth at s_0.

The boundary value problem (2.1) must be completed by boundary conditions. Transport $H\mathbf{u}$ through the boundary vanishes, thus implying

$$\psi = 0, \quad \text{on} \quad \partial\mathcal{D}. \tag{2.3}$$

Since we study topographic waves in an open domain with a boundary line which is not closed, we further require asymptotic conditions. In the case of wave excitation from infinity we state

$$\psi = \text{finite}, \quad \text{as} \quad s \to \infty, \tag{2.4}$$

and, alternatively, if there is no wave source at infinity,

$$\psi \to 0, \quad \text{as} \quad s \to \infty. \tag{2.5}$$

A method was recently presented which economically solves (2.1) subject to (2.3) in a straight, infinite channel; this is described in SH (1986). The idea was to make use of the narrow, elongated shape of the bathymetry. The streamfunction was expanded in terms of a complete function set $\{P_\alpha\}$, according to

$$\psi(s, n) = \sum_{\alpha=1}^{2N} P_\alpha(s, n)\psi_\alpha(s), \tag{2.6}$$

thereby incorporating all functional dependence on n in the preselected $2N$ basis functions P_α (N symmetric and N skewed with respect to $n = 0$). These can be chosen, for convenience, as trigonometric functions fulfilling (2.3). Each basis function is weighted by a residue function $\psi_\alpha(s)$, which remains to be determined. For a finite order of expansion N we anticipate that (2.6) represents an approximation of the exact solution. With (2.6) the two-dimensional problem (2.1), which

is amenable to an exact solution only for few cases, can be approximated by a system of ordinary differential equations for the residue functions. The system is obtained by a weighted integration of the two-dimensional equation (2.1) over the narrow coordinate n and using the expansion (2.6). This procedure is explained in details in SH (1987b). The following paragraphs give a summary.

In the region ⓞ of the semi-infinite channel the differential equation can be transformed to an algebraic system looking for solutions proportional to $\exp(iks)$, see SH. In this region wave propagation is governed by the dispersion relation in the infinite channel, see inset of Fig. 1. For frequencies below the cutoff frequency σ_0 the dispersion relation takes the well-known form of topographic or shelf waves propagating in either channel direction (along either shore line). These waves are right-bounded on the Northern Hemisphere. For $\sigma > \sigma_0$ wavenumbers are complex and the waves exhibit exponentially growing or decreasing amplitudes in space. Consequently, solutions in infinite domains can not be constructed. In a semi-infinite or finite region, however, these solutions may well represent physically reasonable solutions.

In region ⓪, however, the system of ordinary differential equations must be integrated numerically using a 4th-order Runge-Kutta scheme because its coefficient matrices depend on the coordinate s. This is due to a varying thalweg depth $h(s)$ modeled by

$$h(s) = \begin{cases} \begin{cases} \eta + \sin^p\left(\dfrac{\pi s}{2s_0}\right), & 0 < s < s_0, \quad p \geqslant 2 \\ \eta + 1 - \sin^{-p}\left(\dfrac{\pi(s_0 - s)}{2s_0}\right), & \\ \qquad\qquad 0 < s < s_0, \quad p \leqslant -2 \end{cases} \\ \eta + 1, \quad s > s_0. \end{cases} \tag{2.7}$$

Profiles for different values of the longitudinal topography parameter p are illustrated in Fig. 3. The exclusion of $|p| < 2$ provides computational advantages as very large values of the slope parameter $S = h^{-1}(dh/ds)$ in the neighborhood of $s = 0$ and $s = s_0$ are avoided this way. A considerable simplification is achieved with B = constant; the estuary has then the shape of an open rectangle.

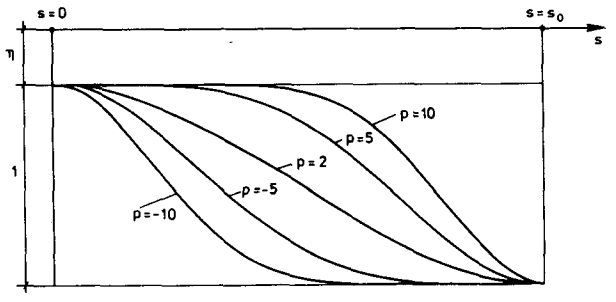

FIG. 3. Thalweg depth profiles for different values of the longitudinal topography parameter p.

The solution in the domain $\mathcal{D}$ can be written as

$$\psi = \begin{cases} \psi^0, & 0 < s < s_0 \\ \psi^\infty, & s > s_0, \end{cases} \tag{2.8}$$

where ψ^0 and ψ^∞ are subject to the appropriate boundary conditions (2.3)–(2.5). In the far field region ψ^∞ will be a superposition of the incident topographic wave mode and a *series* of reflected modes of the same frequency, viz.

$$\psi^\infty = \psi_i^\infty + \sum_{\gamma=1}^{2N} D_\gamma \psi_\gamma^\infty. \tag{2.9}$$

We select the wavenumber k_i of the incident mode such that the group velocity vector $\mathbf{c}_{gr}$ points towards the bay opposite to that of the reflected modes with real wavenumbers k_γ. Modes with complex wavenumbers are allowed to contribute to the far field provided that $\mathrm{Im} k_\gamma > 0$ and they decay exponentially towards infinity. These requirements select $2N$ possible from $4N$ available wavenumbers. Here ψ_i^∞ and ψ_γ^∞ can be readily calculated using the methods developed for the infinite channel, whereas ψ^0 and D_γ remain as unknowns.

At s_0, where ψ^0 and ψ^∞ are patched together, both ψ and $\partial\psi/\partial s$ must be continuous. These two conditions for each spectral component ψ_α eventually allow calculation of ψ^0 and D_γ. For details of the numerical procedure and the determination of the unknowns the reader is referred to SH (1987b).

3. Reflections of topographic waves

This section essentially follows SH (1987b), however, a less restricted thalweg profile is studied and parameter dependencies are given.

a. Reflection patterns in a model N = 2

We learn from (2.8) that $2N + 1$ modes are superposed which make up the solution ψ^∞ far away from the reflecting zone. It is of particular interest to determine the reflection coefficients R_γ corresponding to the individual modes with wavenumber k_γ. Usually, these are calculated with the help of an energy argument; R_γ then is proportional to the averaged total energy flux contained in the mode κ_γ. Indeed, from the potential vorticity equation of which (2.1) represents the time-free form, a conservation equation for the kinetic energy of the depth averaged (barotropic) velocity field can be deduced. This equation contains the divergence of the flux of topographic wave energy, see Johnson (1988) for details.

Here, however, the strength of the contributing

modes is estimated by scaling the maximum value of the modulus of the streamfunction ψ_γ^∞ over the width with the maximum value of that of the incident mode ψ_i^∞. More precisely, we define

$$R_\gamma = \frac{\max_n |D_\gamma \psi_\gamma^\infty|}{\max_n |\psi_i^\infty|}. \quad (3.1)$$

Figure 4 shows R_γ of the two possible reflected modes as functions of the frequency. The reflected modes are induced by the incident mode ■ which has $c_{gr} \uparrow\uparrow c_{ph}$ towards $s = 0$.

When solving for ψ two cases have to be considered. If $\sigma > \sigma_0$ there exist no modes with $\mathrm{Im}k = 0$ and we cannot define an incident mode as in (2.9). Setting $\psi_i^\infty = 0$ renders the algebraic system, which determines ψ^0 and D_γ, homogeneous. Nontrivial solutions can be found, if ever, for distinct frequencies for which the system would become singular. On the other hand, for $\sigma < \sigma_0$, the system is inhomogeneous and can be inverted.

Calculations have shown that there are indeed real frequencies producing nontrivial solutions. Thus, there exists a *discrete spectrum* for $\sigma > \sigma_0$ and a *continuous spectrum* for $\sigma < \sigma_0$. The contour lines of the streamfunction ψ for different frequencies are also plotted in Fig. 4. Corresponding to the established terminology used in quantum mechanics we may call the waves which belong to the discrete *bound states* of topographic waves in the semi-infinite channel whereas the waves $\sigma < \sigma_0$ are *free states*. The terminology is very appealing and obviously applies here well, as inspection of the streamfunctions in Fig. 4 reveals. The patterns also show that for types 1 and 2, and type 3 with larger frequencies, the use of a linear theory is justified.

The bound states must be identified with the type-2 waves, bay-modes, reported in SH (1987a) and summarized in the introduction. Indeed, the frequencies $\sigma = 0.395$ are the same and, when ignoring in the rectangle the streamfunction at the far end, the mode structures are alike, see Figure 1. We therefore conclude that the occurrence of the bay-mode in the rectangular basins for $\sigma > \sigma_0$ is due to two trapped bound states of topographic waves in either lake bay. The streamfunction of this mode consists of $2N$ modes with $\mathrm{Im}k_\gamma > 0$ for $s > s_0$ and is spatially evanescent. The longer a lake basin is, the weaker will be the coupling of the bound modes in the respective bays.

Starting from σ_0 and decreasing σ we observe that the wave pattern undergoes considerable alterations which correspond to changes in the relative strength of the two reflected modes. Close to the critical frequency σ_0, energy is distributed among several modes whereas for other frequencies most of the reflected energy is contained in the ●-mode. This is the mode with the negative of the incident wavenumber. More precisely, as $R_\circ$ decreases $R_\bullet$ increases. For $\sigma < 0.25$ $R_\circ$ oscillates weakly while gradually decreasing and $R_\bullet > 0.98$. This can be verified by considering the associated streamfunctions. For $0.254 < \sigma < \sigma_0$ the reflected wave mainly consists of the ○-mode. What evolves is a beat pattern at the same channel side where the incident mode propagates. The increase of $R_\bullet$ manifests itself as a growing leakage of wave activity into the opposite channel side, because the ●-mode has $k = -k_i$. For $0.120 < \sigma < 0.254$ $R_\bullet$ is dominant, and this is clearly visible in the wave patterns. The dispersion relation has $\partial\sigma/\partial k > 0$ for this reflected mode and consequently, increasing wavelengths accompany decreasing frequencies.

At $\sigma = 0.115$ a remarkable resonance is discovered: Two coinciding peaks give rise to a local minimum and maximum for $R_\bullet$ and $R_\circ$, respectively. Looking at the wave pattern suggests that this again is a bay-trapped mode. Contrary to the trapped modes with $\sigma > \sigma_0$, which are true bound states, this mode has also a nonvanishing periodic contribution in $s > s_0$. The pattern is, however, a bay-mode or type-2 wave because the characteristic structure is due to the modes with $\mathrm{Im}k_\gamma > 0$ belonging to the second-mode unit which still has a complex branch for $\sigma_1 < \sigma < \sigma_0$ (see inset).

The resonance $\sigma = 0.115$ coincides with an eigenfrequency in the closed basin as indicated with ▲. The structure agrees well with that shown in Fig. 1. Below this resonance the component $R_\bullet$ dominates $R_\circ$ again and large-scale topographic waves are observed. There is a further resonance at $\sigma = 0.088$. For $\sigma < \sigma_1$ all modes have $\mathrm{Im}k_\gamma = 0$ in this second-order model and no further bay-modes can be expected. Instead of this, contributions of the real branch belonging to the second mode unit are possible. More quantitative statements, however, can not be made and models with $N = 3, 4, 5, \cdots$ would have to be investigated.

b. *Topographic waves in Lake Lugano*

Interpretation of the long-periodic signals of the order of 70 to 80 hours observed in Lake Lugano (northern basin) was puzzling for a long time. Mysak et al. (1985) propose that the wave motion is a fundamental Ball-mode. Johnson (1987b), using the same elliptical basin with a realistic aspect ratio, concludes, due to the strongly U-shaped transverse depth profiles, that it is rather a mode with a frequency close to the cutoff and a large along-axis wavenumber. A third interpretation arose when solving (2.1) by a finite element procedure, Trösch (1984). In the period range 65 to 100 h rather small scale and bay-trapped wave patterns evolve. The nature and properties of the latter were not understood, but a qualitative comparison of these findings with the streamfunction patterns in the straight, semi-infinite channel brings clarification, see Fig. 5. For this comparison a highly idealized configuration is used. Effects of curvature are small (Stocker, 1987) and need not be considered. Bay-modes are seen

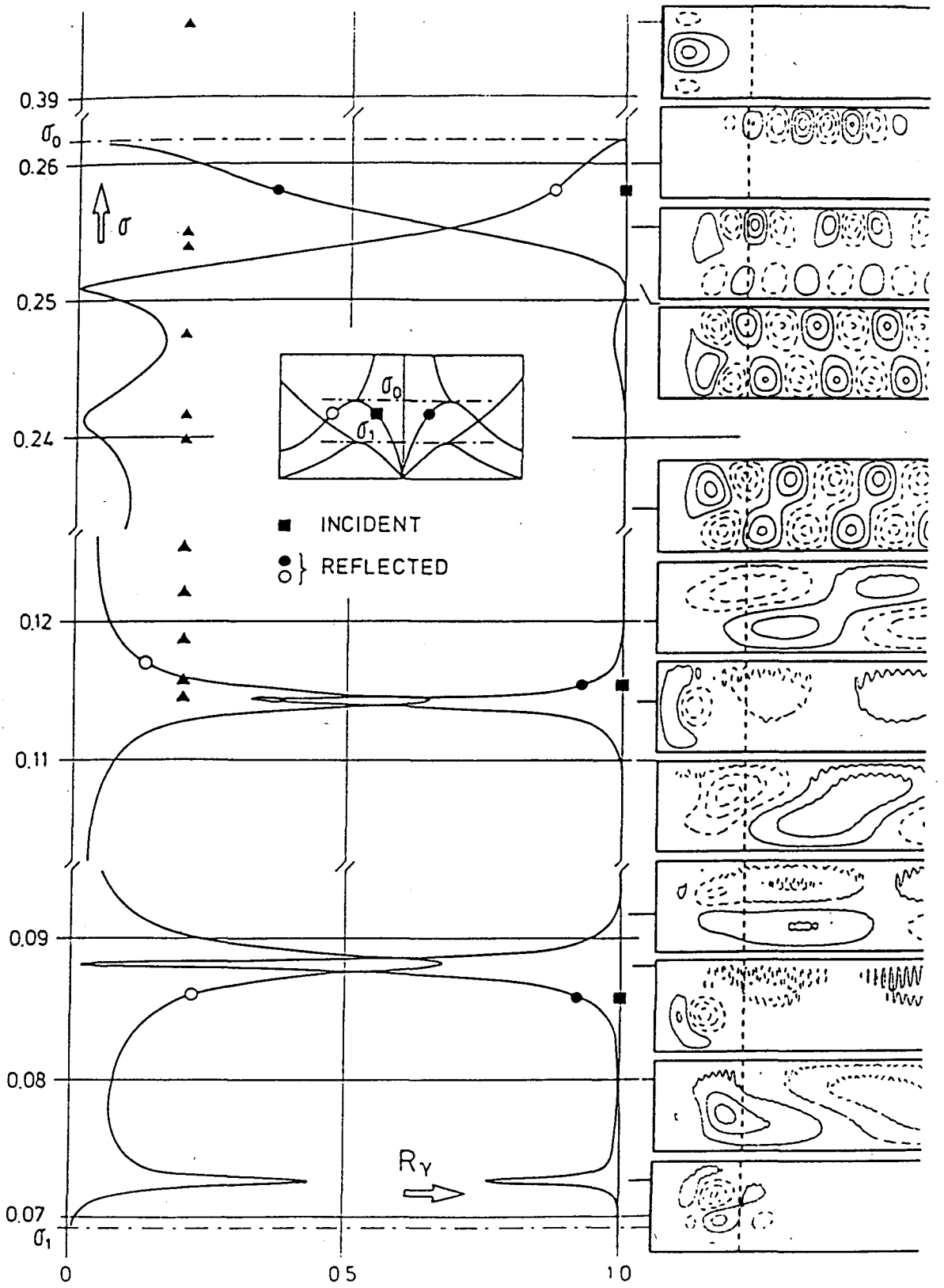

FIG. 4. Reflection coefficients and streamfunction patterns in subdomains of the frequency interval $[\sigma_1, \sigma_0]$ of the two reflected modes ● and ○, respectively. The coefficient of the incident mode ■ is scaled to 1 and both c_{gr} and c_{ph} are directed towards the reflecting shore. ▲ indicate lake solutions for $\sigma > 0.11$ corresponding to Fig. 1. The inset explains the position of the modes within the dispersion relation and the parameters are $N = 2$, $s_0 = 1$ (dashed line), $q = 2$, $\epsilon = 0.05$, $p = 2$, $\eta = 0.01$. (From Stocker and Hutter, 1987b.)

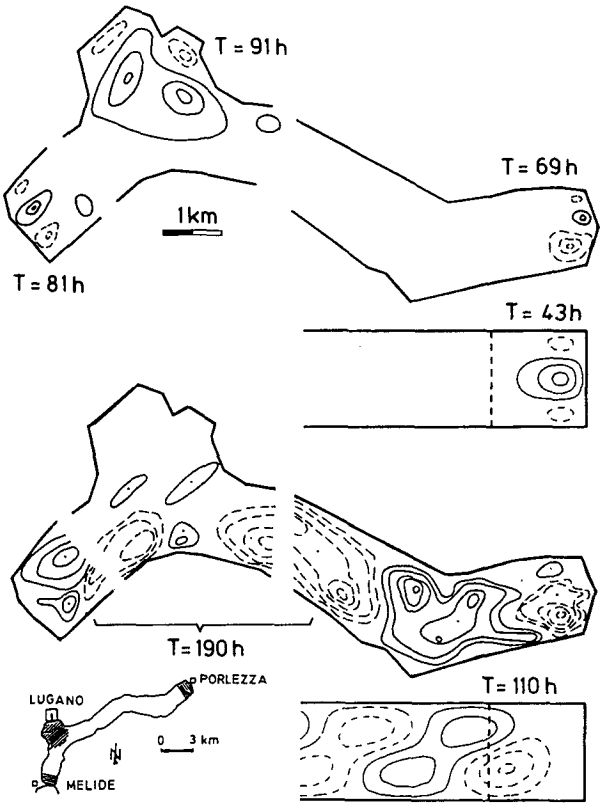

FIG. 5. Qualitative comparison of finite element results of long periodic wave motion in the northern basin of Lake Lugano with results in the rectangular semi-infinite channel. Periods of the latter are smaller because a longitudinal shore topography with a smaller slope than in the finite element basin was chosen.

to be sustained independently in the three bays of Porlezza, Melide and Lugano. The basin is sufficiently elongated such that the coupling of the individual modes is negligible. At $T = 190$ h a basin wide eigenmode occurs which can be related to a channel-mode with $\sigma < \sigma_0$, see also Fig. 1.

This new result is of importance particularly for elongated lakes with very steep transverse topography implying a small cutoff frequency. Let us estimate the frequency of the quadratic Ball-mode using the model of Ball (1965). With an aspect ratio of 1.5/17 = 0.088 we obtain the estimate of $T = 350$ h. Recall that the transverse depth profiles are steeper than the parabolic of Ball's elliptic basin. Periods would have to be even longer. Measurements, however, clearly point at roughly 70 to 80 hours being close to, or rather above, the cutoff frequency of this channel-shaped basin. It is thus reasonable that the signal could be the trace of a bay-trapped topographic wave of one of the bays. For constant s_0 only the topography parameters p and q determine the frequency of the bay-mode. Decreasing p lowers σ considerably. So a bay-mode with $\sigma = 0.395$, $T = 43$ h can easily brought into the correct range. A further argument supporting this interpretation is the fact that spectral peaks of temperature time series from Porlezza and Melide do not exactly coincide. This difference is likely to be due to two *independent* bound modes at the two lake ends. Giving a final answer would require data which would uncover the spatial structure much more clearly than can be done with the data at hand.

c. *Parameter dependence*

We now investigate the influence of the geometry of the bay on the reflection of topographic waves. The bathymetry of the bay-zone is described by the longitudinal and transverse topography parameters p and q. Previous studies revealed the pronounced dependence of the dispersion relation on q. Generally, an increase of q, while holding the side wall parameter ϵ constant, causes a decrease of both cutoff frequencies σ_0 and σ_1, see Table 1. For the tested parameter domain, $-5 \leqslant p \leqslant 5$ and $0.5 \leqslant q \leqslant 5$, the qualitative structure depicted in Fig. 4 is preserved. It is the position of the resonances which changes with p and q.

Figure 6 displays σ of the resonances or type-2 waves as a function of q when p is constant. Increasing q, i.e. more concave depth profiles with steeper slopes, increases these frequencies. Changes are, however, small. Although the profiles alter their shape from $q = 2$ to 5 considerably the associated periods ($T = 16.9$ h/σ) only vary from 132 to 147 h. For $q \leqslant 1.5$ no resonances can occur in this second order approximation because the cutoff frequency is too large. The effect is reversed when $q \leqslant 1$, i.e. for convex profiles.

In Figure 7 the influence of p, the longitudinal topography parameter, is studied. The case $p < -2$ models troughlike thalweg profiles. For these, increasing steepness causes bay-mode frequencies to slightly decrease. Shelflike profiles with $p > 2$ have strongly increasing frequencies of the resonances as p is growing. The top curve shows the bay-mode with $\sigma > \sigma_0$ whereas the lower two curves describe the resonances in $\sigma_1 < \sigma < \sigma_0$.

Comparing Figs. 6 and 7 demonstrates that for type-2 waves p is the dominating parameter, i.e. primarily, the thalweg profile governs the frequency of the resonance. On the other hand, the structure of the dispersion relation and mainly the values of σ_0 and σ_1 are dictated by q.

TABLE 1. Cutoff frequencies of the first (σ_0) and the second (σ_1) mode unit for various values of the transverse topography parameter q; $N = 2$, $\epsilon = 0.05$.

	q					
	0.5	1	2	3	4	5
σ_0	0.342	0.305	0.261	0.225	0.193	0.167
σ_1	0.182	0.138	0.069	0.035	0.018	0.010

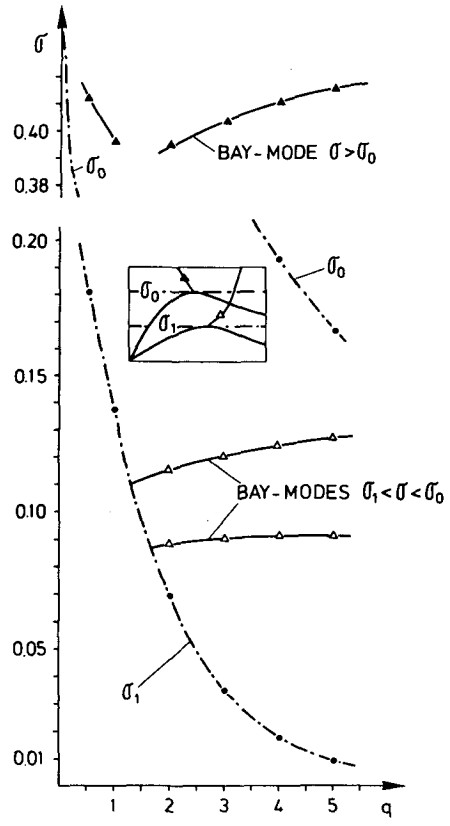

FIG. 6. Frequencies of the resonances or bay-modes in $\sigma_1 < \sigma < \sigma_0$ and a bay-mode with $\sigma > \sigma_0$ as functions of the transverse topography parameter q; $N = 2$, $\epsilon = 0.05$, $p = 2$, $\eta = 0.01$. The cutoff frequencies for the two mode units are indicated.

d. *Wave reflection and modal types*

So far, we have studied the reflections of topographic waves, when the incident mode belongs to the first mode unit and has $c_{gr} \uparrow\uparrow c_{ph}$ towards the reflecting zone. We also investigated the situation for an incident mode with $c_{gr} \uparrow\downarrow c_{ph}$. For this case, the graph of Fig. 4 qualitatively looks the same except that the curves R_O and $R_\bullet$ are interchanged. The position of the two conspicuous resonances is unchanged.

Figure 8 summarizes the results of importance. The incident mode with $c_{gr} \uparrow\downarrow c_{ph}$ in the right column of Fig. 8 has its wave crests at the opposite side of the channel. Energy is propagating towards s_0 whereas the phase propagates away from it. These two cases distinguish two different types of reflection patterns, type 1 and type 3. Type 1 has a large scale structure with increasing wave lengths for decreasing σ. Conversely, type 3 exhibits a small scale pattern which is intensified for decreasing frequencies. The distinction of these types and their individual properties agree with the classification presented in SH (1987a). There, we only were able to make the distinction plausible by phenomenological arguments. We now have discovered a physical explanation for the occurrence of bay-modes, Ball-modes and channel-modes in enclosed basins. Comparing Fig. 8 with Fig. 1 makes it clear:

(i) The type-1 modes or Ball-modes originate from a sequence of reflections at the lake ends which are induced by an incident wave with $c_{gr} \uparrow\uparrow c_{ph}$. For an appropriately selected frequency, i.e. the eigenfrequency, the pattern is not evanescent in time and a Ball-mode is sustained.

(ii) The basin solutions classified as type 2 or bay-modes are due to the conspicuous resonances observed in Fig. 4. As Fig. 8 demonstrates the structure in the bay is only weakly influenced by the incident mode.

(iii) Finally, the channel-modes or type-3 waves of Fig. 1 can be explained as the result of a sequence of reflections at the lake ends which are induced by a mode with $c_{gr} \uparrow\downarrow c_{ph}$. Contrary to the Ball-modes, the spatial scale decreases with decreasing frequency.

These results provide a more precise and broader understanding of topographic waves in channels and lakes. It is now clear that demonstrated solutions of the exact models do not exhibit the complete variability of solutions. The existence of three distinctly different wave types is a natural consequence of the typical structure of the dispersion relation. The conspicuous

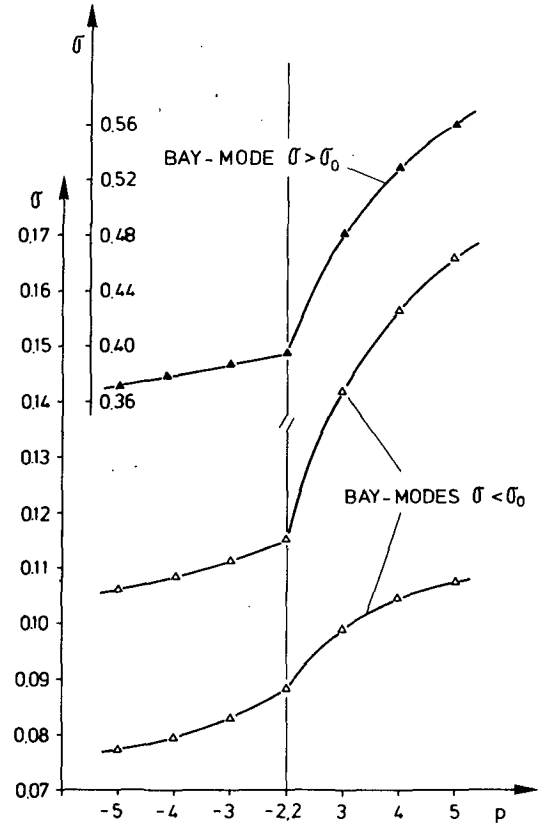

FIG. 7. Frequencies of the resonances or bay-modes in $\sigma_1 < \sigma < \sigma_0$ and a bay-mode with $\sigma > \sigma_0$ as functions of the longitudinal topography parameter p; $N = 2$, $q = 2$, $\epsilon = 0.05$, $\eta = 0.01$.

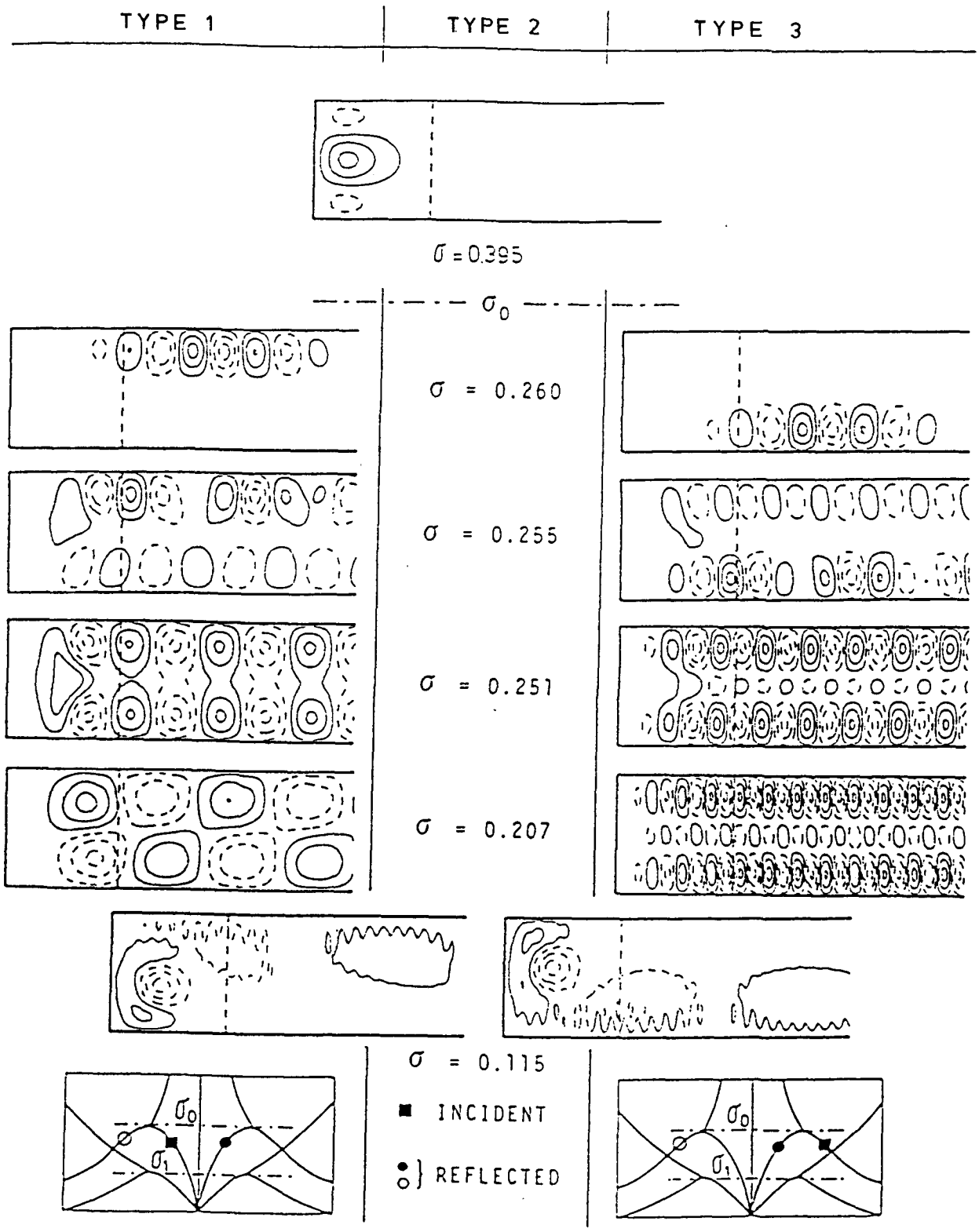

FIG. 8. Reflection patterns induced by an incident wave with $c_{gr} \uparrow\uparrow c_{ph}$ (type 1), and $c_{gr} \uparrow\downarrow c_{ph}$ (type 3), respectively. The modes at the resonance $\sigma = 0.115$ and $\sigma = 0.395$ are of type 2. The parameters are as in Fig. 4. (From Stocker and Hutter, 1987b, with modifications.)

eigenmodes in the rectangular basin can be understood in terms of reflections of topographic waves at either shore zone. Depending on the structure of the incident wave the corresponding type is established. All parameter dependencies are explicable with the help of this correspondence.

4. Conclusions

In this paper we studied the motion of topographic waves in channels as they propagate towards a shore-zone. The potential vorticity equation was approximately solved by assuming the transverse modal structure to be expressible in terms of a few basis functions. The two-dimensional boundary value problem was therefore reduced to a system of coupled one-dimensional problems to which high accuracy integration routines can be applied.

In the bay-zone the wave field consists of modes with real and complex wavenumbers and streamfunctions of the far field are periodic (for external harmonic forcing) or evanescent in space (for no forcing). In the process of reflection the incident energy is distributed among possible reflected modes with different wavelengths. They form a reflection pattern which is characteristic of the incident mode and the excitation frequency. At distinct frequencies the estuary exhibits a resonant behavior. A small excitation from infinity causes pronounced wave activity in the shore zone. This wave motion remains trapped in the channel end.

It came as a surprise that above the cutoff frequency nontrivial solutions are possible, which decay exponentially towards infinity. These are true bound states of the system and coincide with the bay-modes of the closed basin. The semi-infinite channel, therefore, discloses a spectrum consisting of a continuous and a discrete part which join at the cutoff frequency.

The existence of bay-trapped modes also has bearings on the interpretation of observations. The finite element solutions of Lake Lugano, which were thought to contradict the existing exact solutions and related interpretations turn out to be most likely the bay-modes of this natural basin.

Further investigations are required. In many cases, enclosed basins are connected with the open ocean by an estuary. It is likely that the estuary can act as a geometry that restores and transmits wave energy from the ocean. At present, very little is known about this interaction. A study addressing these questions is in preparation (Stocker and Johnson, 1988a).

Stocker and Johnson (1988b) calculate solutions of (2.1) for a semi-infinite channel with a simple bottom topography. It is shown that both bay-modes and resonances are reminiscent features of topographic waves in an open domain. Another more general way to proceed would be to investigate the mathematical properties of the partial differential operator (2.1) by the methods of linear functional analysis. Are there any criteria such that this operator has a continuous and a discrete spectrum? What is the structure of the spectrum?

Hence, interpretations of long periodic signals in enclosed and semi-enclosed areas should take into account the existence of bay-trapped vortex modes.

Acknowledgments. I appreciated many fruitful and helpful discussions with K. Hutter. The drawings by I. Wiederkehr are gratefully thanked.

REFERENCES

Ball, F. K., 1965: Second class motions of a shallow liquid. *J. Fluid Mech.*, **23**, 545–561.

Brown, P. J., 1973: Kelvin wave reflection in a semi-infinite canal. *J. Mar. Res.*, **31**, 1–10.

Johnson, E. R., 1987a: Topographic waves in elliptical basins. *Geophys. Astrophys. Fluid Dyn.*, **37**, 279–295.

——, 1987b: A conformal mapping technique for topographic wave problems: semi-infinite channels and elongated basins. *J. Fluid Mech.*, **177**, 395–405.

——, 1988: Topographic waves in open domains. Part I: Boundary conditions and frequency estimates. *J. Fluid Mech.*, submitted.

Mysak, L. A., 1980: Recent advances in shelf wave dynamics. *Reviews of Geophysics and Space Physics*, **18**, 211–241.

——, G. Salvade, K. Hutter and T. Scheiwiller, 1985: Topographic waves in an elliptical basin, with application to the Lake of Lugano. *Phil. Trans. R. Soc. London*, **A316**, 1–55.

Stocker, T., 1987: Topographic waves: Reflections and eigenmodes in lakes and semi-infinite channels. *Mitteilungen der Versuchsanstalt für Wasserbau, Hydrologie und Glaziologie, ETH Zürich*, Nr. 93.

——, and K. Hutter, 1986: One-dimensional models for topographic Rossby waves in elongated basins on the *f*-plane. *J. Fluid Mech.*, **170**, 435–459.

——, and ——, 1987a: Topographic waves in rectangular basins. *J. Fluid Mech.*, **185**, 107–120.

——, and ——, 1987b: Topographic waves in channels and lakes on the *f*-plane. *Lecture Notes on Coastal and Estuarine Studies*, Vol. 21, Springer.

——, and E. R. Johnson, 1988a: Reflection and transmission of shelf waves in a shelf-estuary system. *J. Phys. Oceanogr.* (in preparation).

——, and ——, 1988b: Topographic waves in open domains. Part II: Bay-modes and resonances. *J. Fluid Mech.* (submitted).

Taylor, G. I., 1920: Tidal oscillations in gulfs and rectangular basins. *Proc. London Math. Soc.*, **20**, 148–181.

Trösch, J., 1984: Finite element calculation of topographic waves in lakes. *Proc. of Fourth Int. Conf. on Applied Numerical Modeling*, Tainan, Taiwan.